IDENTIFYING ISOTROPIC EVENTS USING A REGIONAL MOMENT TENSOR INVERSION

Douglas S. Dreger[1], Sean R. Ford[2], and William R. Walter[2]

Berkeley Seismological Laboratory[1] and Lawrence Livermore National Laboratory[2]

Sponsored by the National Nuclear Security Administration

Award No. DE-FC52-06NA27324[1] and DE-AC52-07NA27344[2]
Proposal No. BAA06-42

ABSTRACT

In our previous work the deviatoric and isotropic source components for 17 explosions at the Nevada Test Site (NTS), as well as 12 earthquakes and 4 collapses in the surrounding region of the western U.S., were calculated using a regional time-domain full waveform inversion for the complete moment tensor (Dreger et al., 2008; Ford et al., 2008; Ford et al., 2009a). The events separate into specific populations according to their deviation from a pure double-couple and ratio of isotropic to deviatoric energy. The separation allows for anomalous event identification and discrimination between explosions, earthquakes, and collapses. Confidence regions of the model parameters are estimated from the data misfit by assuming normally distributed parameter values. We developed a new Network Sensitivity Solution (NSS) in which the fit of sources distributed over a source-type plot (Hudson et al., 1989) show the resolution of the source parameters. The NSS takes into account the unique station distribution, frequency band, and signal-to-noise ratio of a given event scenario. The NSS compares both a hypothetical pure source (for example an explosion or an earthquake) and the actual data with several thousand sets of synthetic data from a uniform distribution of all possible sources. The comparison with a hypothetical pure source provides the theoretically best-constrained source-type region for a given set of stations, and with it one can determine whether further analysis with the data is warranted. We apply the NSS to a NTS nuclear explosion, and earthquake, as well as the 2006 North Korean nuclear test, and a nearby earthquake. The results show that explosions and earthquakes are distinguishable; however the solution space depends strongly on the station coverage. Finally, on May 25, 2009, a second North Korean test took place. Our preliminary results show that the explosive nature of the event may be determined using the regional distance moment tensor method. Results indicate that the 2009 event is approximately 5–6 times larger than the earlier test, with an isotropic moment of about 1.8e+22 dyne cm. We perform a series of inversions for pure double-couple, pure explosion, combined double-couple and explosion, full moment tensor, and damped moment tensor inversions to assess the resolution of the isotropic moment of the event.

OBJECTIVES

We build on our previous work to implement the time-domain full-waveform inversion of regional data for the complete moment tensor for source-type identification and discrimination (Dreger et al., 2008; Ford et al., 2008) to develop a method of assessing uncertainty in solutions due to the recording geometry. By means of forward calculations the fit of thousands of possible moment tensor solutions, distributed over a Hudson et al. (1989) source-type plot, the classification of a given seismic event in terms of double-couple, non-double-couple, and isotropic components can be more thoroughly examined. Direct comparisons between the fit of such mechanisms can greatly aide in the classification of event type, and importantly present it in a manner that allows for the assessment of solution resolution and uncertainty in terms of station geometry.

RESEARCH ACCOMPLISHED

Introduction

Ford et al. (2009a) calculated seismic moment tensors for 17 nuclear test explosions, 12 earthquakes, and 3 collapses in the vicinity of the NTS in the Western U.S. They found that the relative amount of isotropic and deviatoric moment provided a good discriminant between the explosions and earthquakes. The observational work to describe the discriminant was accompanied by a theoretical study into the sensitivities of the method and it was found that the ability to resolve a well-constrained solution is dependent on station configuration, data bandwidth, and signal-to-noise ratio (SNR). It is difficult to state steadfast rules for what source-types can be resolved for all conditions, when different conditions lead to different levels of confidence in the solution. Therefore, in this study we develop a confidence analysis specific to the source type, station configuration and data SNR, which we call the network sensitivity solution (NSS).

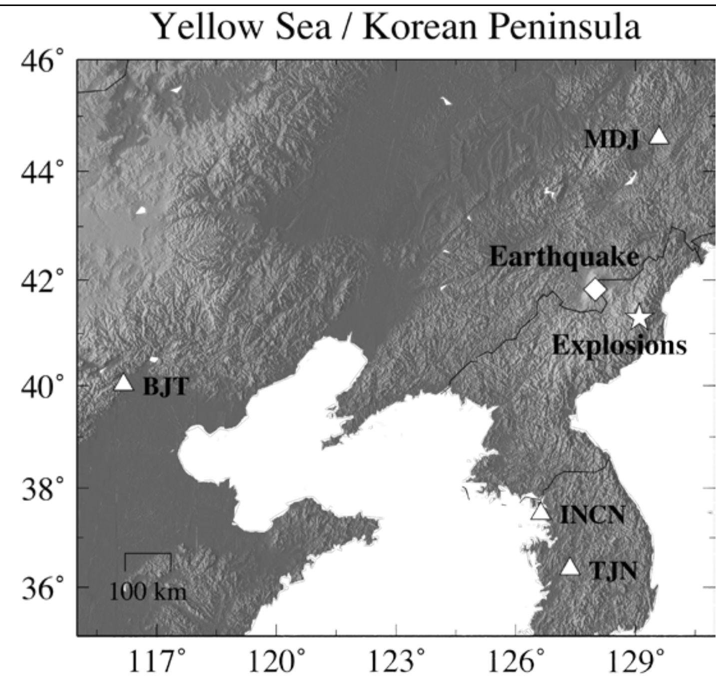

Figure 1. Map of the Yellow Sea / Korean Peninsula with the North Korea tests (5-point star) and nearby earthquake (diamond) as well as the stations used in their analysis (triangles).

There have been many attempts to understand error in seismic moment tensor inversions. Sileny and coathors have done extensive sensitivity testing of the methods they use to calculate the moment tensor. Sileny et al. (1992; 1996), Sileny (1998), Jechumtalova and Sileny (2001), and Sileny (2004) have collectively investigated the effects of incorrect event depth, poor knowledge of the structural model including anisotropy, noise, and station configuration on the retrieved solution. They found that for only a few stations with data of SNR>5 the moments of various components were sensitive to improper source depth and velocity model, but that the mechanism remained robust, and that spurious isotropic components may manifest in the solution if an isotropic medium assumption is made incorrectly. Roessler et al. (2007) confirm this last result. The probabilistic inversion method by Weber (2006) using near-field full-waveform data helped to inspire the approach taken in this study. Weber (2006) inverts for hundreds of sources using a distribution of hypocentral location based on *a priori* information. Perturbations to the velocity model and noise are also added in the synthetic portion of the study. Empirical parameter distributions are then produced to assess the resolution. Mechanism distribution is plotted with a Riedesel and Jordan (1989) plot, which is also the preference of many of the previously mentioned studies. In the following study we will employ the source-type plot from Hudson et al. (1989), which is described in Ford et al. (2009a). Further details of the inversion method and its practical implementation are also given in Ford et al. (2009a).

Network Sensitivity Solutions

The theoretical NSS tries to answer the question of how well a pure earthquake or explosion can be resolved with very high SNR data for the given event scenario (i.e., data bandwidth and station distribution). To do this we use the GFs to first produce data for a model event (earthquake or explosion) as well as a uniform distribution of synthetic sources representing all possible sources, where the moment of these sources is chosen so as to best fit the model event data. The source-type parameters (Hudson et al., 1989) are calculated for each of the thousands of synthetic sources (Figure 2a). Since the source-type plot does not account for total seismic moment (only relative moment) or source orientation, a single set of source-type parameters (one point on the source-type plot) can represent several sources. For example, a DC source with any strike, rake, or dip, will plot in the center of the source-type plot (Figure 2b). However, as one moves away from the center of the source-type plot (location of a DC mechanism), source orientation becomes less important to the seismic radiation so that the top and bottom of the plot are uniquely represented by an explosion or implosion, respectively.

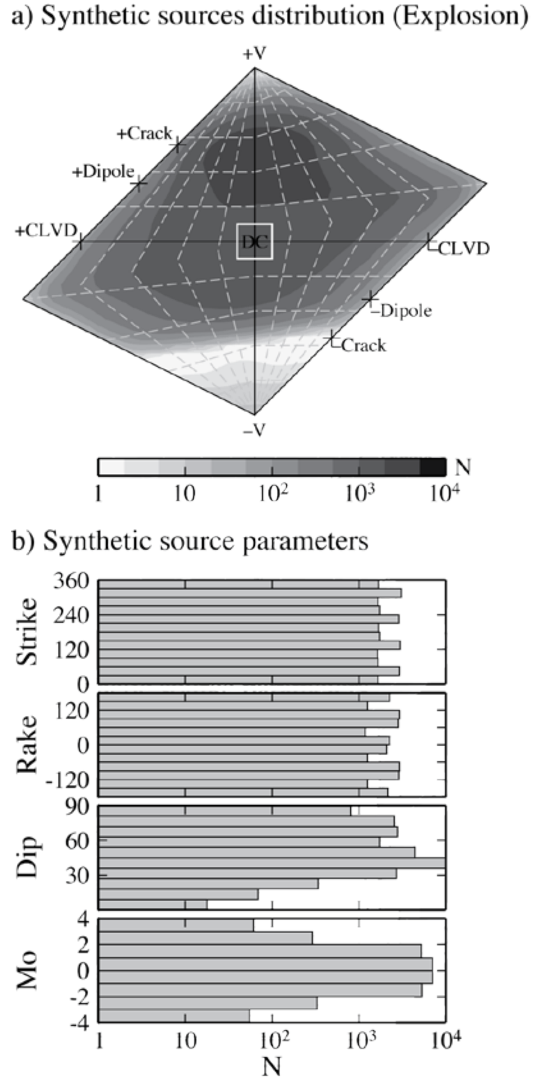

Figure 2. Synthetic sources. a) Source-type plot of synthetic source distribution. Gray scale gives the 0.1-unit smoothed number of events, and the white box outlines the sources described in b). b) Parameters of the synthetic sources contained in the white box in b).

The model event data *d* is then compared with the synthetic source data *s* and the fit for each comparison is quantified by the variance reduction (VR)

$$\mathrm{VR} = \left[1 - \frac{\sum_i (d_i - s_i)^2}{\sum_i d_i^2}\right] \times 100 \,. \tag{1}$$

where *i* are the displacements at all times for all components at all stations.

The VR for each synthetic source is calculated and plotted as a function of source-type parameter on the source-type plot. Since a single set of source-type parameters can represent many sources that could have varying levels of fit to the model event data (and therefore, VR), a moving-maximum window is used to smooth the VR distribution. The source-type plot empirical VR distributions are shown in Figure 2 for a small earthquake located in southeast China.

NSS for a Southeast China Earthquake

Figure 3 gives the theoretical and actual NSSs for the earthquake in China, as well as the waveforms for the data, Best-fit, Example, and Explosion models for comparison. The actual NSS for the earthquake (Figure 3b) shows a well-constrained region similar to the theoretical NSS (Figure 3a). The waveforms of the best-fit model (VR = 67%), shown in Figure 3c, fit the data just as well as a pure DC. This result gives us confidence that the MDJ2 model is a good 1-D approximation of the velocity structure in this region, as the expectation is that the small earthquake should be well represented by a double-couple point-source. Importantly, the analysis also shows that a pure explosion fails to fit the data yielding a best fit variance reduction of only 13%.

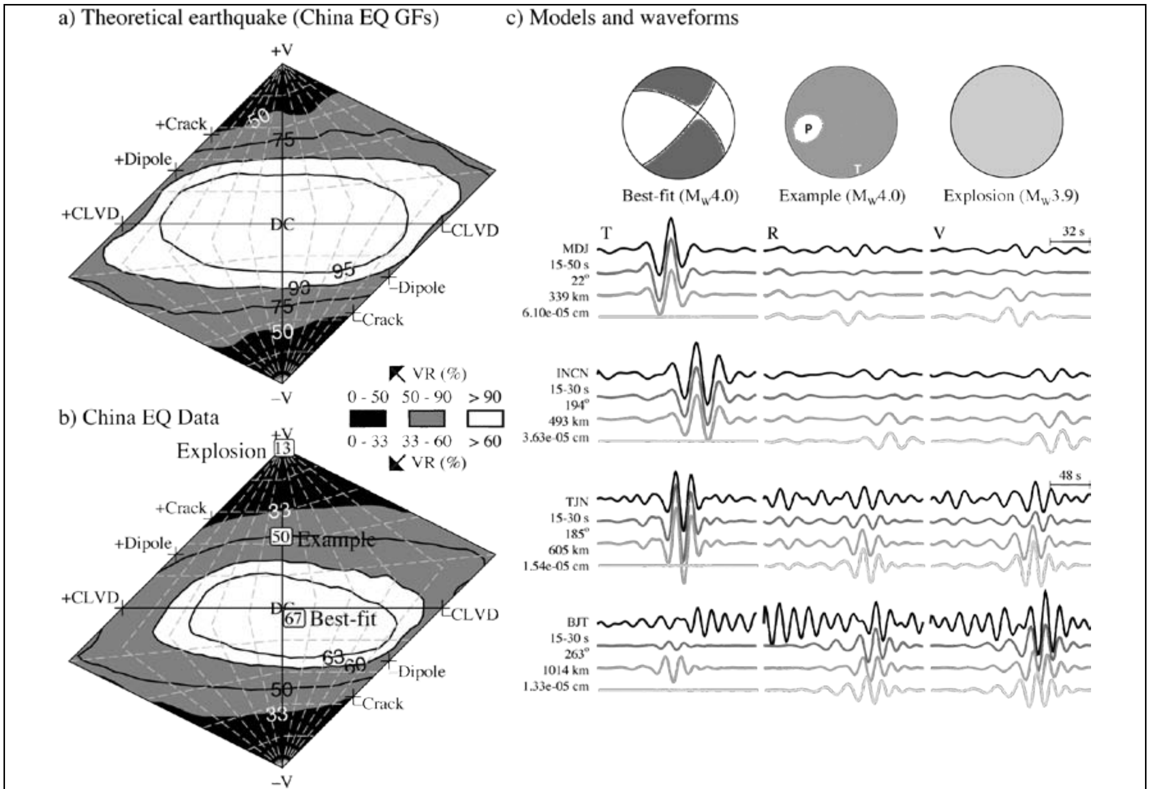

Figure 3. Network sensitivity solution (NSS) for an earthquake (16 Dec 04) near the 2006 North Korea test location. a) Theoretical NSS using one hundred earthquakes with a uniform distribution of fault parameters where the Green's functions are derived from the actual network setup and the data is noiseless. The best-fit model is a pure double-couple (DC) with a VR of 100%. Empirical distributions of other models and the corresponding VR are also given via contours on the source-type plot. b) Actual NSS using data from the China earthquake. The best-fit model with a VR of 67% along with other models and the corresponding VR distributions are shown. For comparison, an Example model (VR = 50%) and a pure Explosion model (VR = 13%) are also plotted and correspond with the models and waveforms given in c). c) Models corresponding to those plotted in b) and their respective forward-predicted waveforms as a function of color compared with the actual waveforms (black line). The left, middle, and right columns are the tangential (T), radial (R), and vertical (V) displacement waveforms, respectively. The text block to the left of the waveforms gives the station name, passband period (s), azimuth, epicentral distance (km), and maximum displacement (cm). The moment magnitudes of the models are also given below the mechanism.

2006 North Korean Nuclear Test

The solution for the October 2006 explosion in North Korea (ODNI, 2006) is much less constrained than the Chinese earthquake due to the simpler radiation pattern. Normally, we would run the inversion without station BJT because the epicentral distance is more than 1000 km and performance of the simpler 1-D velocity model employed here degrades at such great distances. However, preliminary inspection of the theoretical NSS without BJT showed that the solution could not satisfactorily exclude DC sources. Although this understanding could be gained from simple inspection of the station configuration shown in Figure 1b, where without BJT all stations fall along one azimuth with π periodicity (a condition that can always fit the two-lobed Rayleigh radiation pattern of a 45-degree dip-slip mechanism), the example is still instructive for cases that are not so easily visually inspected. With station BJT, the high VR region has the shape typical of NTS events, illustrating the tradeoff between isotropic and vertical, compressive CLVD sources (e.g. Ford et al., 2009b).

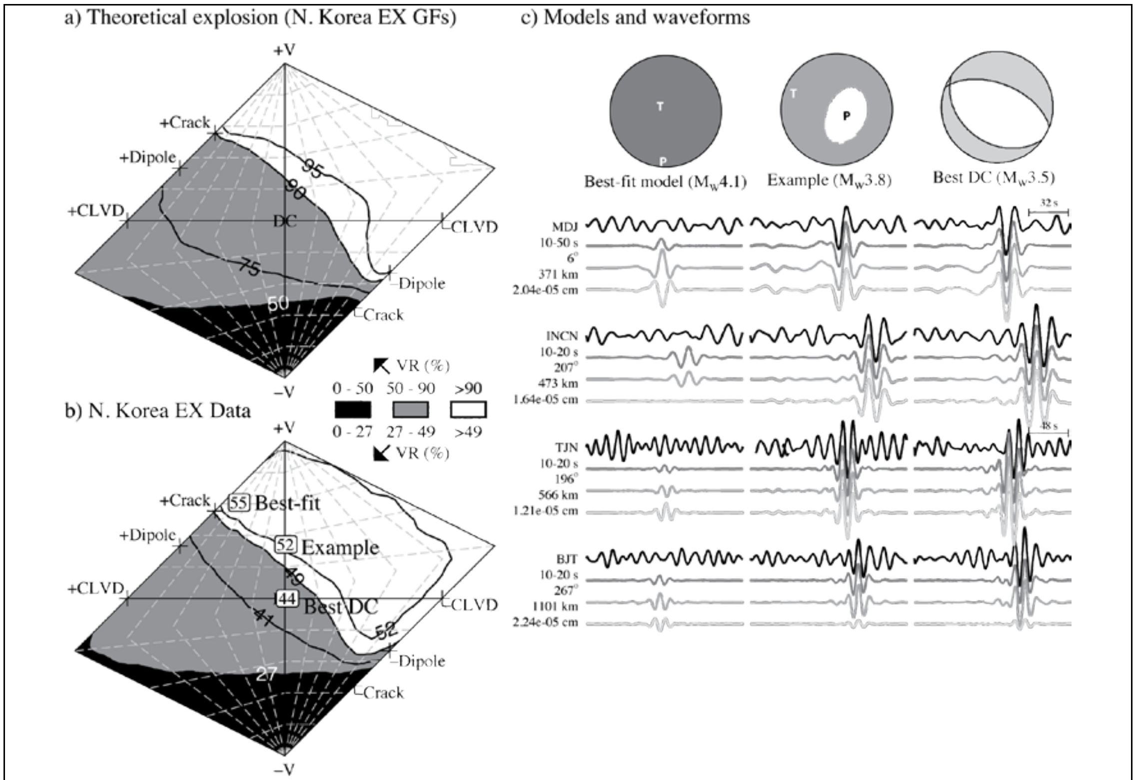

Figure 4. Network sensitivity solution (NSS) for the first North Korea test (9 Oct 06, m_b4.2). a) Theoretical NSS for an explosion where the Green's functions are derived from the actual network setup and the data is noiseless. The best-fit model is an explosion with a VR of 100%. Empirical distributions of models and their corresponding VR are also given via contours on the source-type plot. b) Actual NSS using data from the North Korea test. The best-fit model with a VR of 55% along with other models and the corresponding VR distributions is shown similar to a). For comparison, an Example (VR = 52%) and a Best DC model (VR = 44%) are also plotted and correspond with the models and waveforms in c). c) Models corresponding to those plotted in b) and their respective forward-predicted waveforms as a function of color compared with the actual waveforms (black line). The left, middle, and right columns are the tangential (T), radial (R), and vertical (V) displacement waveforms, respectively. The text block to the left of the waveforms gives the station name, passband period (s), azimuth, epicentral distance (km), and maximum displacement (cm). The moment magnitudes of the models are also given below the mechanism.

The addition of station BJT presents some additional problems for the actual NSS (Figure 4b). BJT is more than 1100 km away from the source, yet the displacement (2.24e-05 cm) is larger than that of station MDJ (2.04e-05 cm), which is only 371 km from the source. The usual method of weighting the data as a function of inverse distance caused the data from BJT to dominate the inversion, since there is only one station at this very great distance. As a corrective measure, we decreased the weight of data from BJT and produced the actual NSS in Figure 4b. As was stated in the discussion of the theoretical NSS, BJT is instrumental in constraining the source to be non-DC. Figure 4c shows that the Best DC model does not produce the observed Rayleigh amplitudes at BJT. Further, there is added confidence that the source is dominantly explosive because the Example mechanism, which fits the waveforms at a VR that is 3% less than the Best-fit model, produces a Love wave that is not observed at MDJ (Figure 4c).

2009 North Korean Test

The pure explosion model for the 2009 test is able to fit the waveforms with a variance reduction of 75% and yields an isotropic moment of 1.8e22 dyne-cm (M_W4.1; all seismic moment values are calculated with the method of Bowers and Hudson, 1999). In contrast, the pure DC solution fits the data much worse at 52% with M_0 = 3.8e22 dyne-cm (M_W4.4). The fact that the single degree of freedom explosion model fits so much better than the four degree of freedom DC model is highly significant and indicates that such a comparison can be a useful discriminant. The strike, rake, and dip of the best-fit DC is 50˚, -85˚, and 10˚. Such a steep dip-slip mechanism is very rare and of all sources calculated by the Global CMT Project (globalcmt.org) less than 1.6% have dips less than 10˚. This type of information can be used as an additional flag for anomalous sources. The differences in the fits between explosion (Best-iso) and DC (Best-DC) sources can be viewed in Figure 5b, where the DC overpredicts the Love wave amplitude at almost all stations and underpredicts the Rayleigh wave amplitudes, especially at station INCN.

Comparisons of waveforms and spectra for the 9 October 2006 nuclear test and 2009 event indicates that the 2009 event is approximately 5.7 times larger than the 2006 event. The isotropic moment for the 2006 event was found to be 0.3e22 dyne-cm (Walter et al., 2007), which agrees with the Koper et al. (2008) value. Therefore, from the waveform comparison the 2009 event should be approximately 1.5e22 to 2.1e22 dyne-cm (scale factor of 5 to 7), which is close to the pure explosion result (1.8e22 dyne-cm) obtained from waveform modeling. Figure 5 shows the raw waveforms at station MDJ for both the 2006 and 2009 North Korea events filtered between 10 and 50 sec. Note that the azimuth to MDJ is 6˚, so the east-west and north-south components are effectively naturally rotated to the tangential and radial directions, respectively. When the waveforms of the 2006 test are magnified by a factor of six, the north-south and vertical components are very similar to the 2009 event. However, the tangential energy that is clear in the 2009 event due to the high SNR is still too small to peak above the noise in the 2006 event.

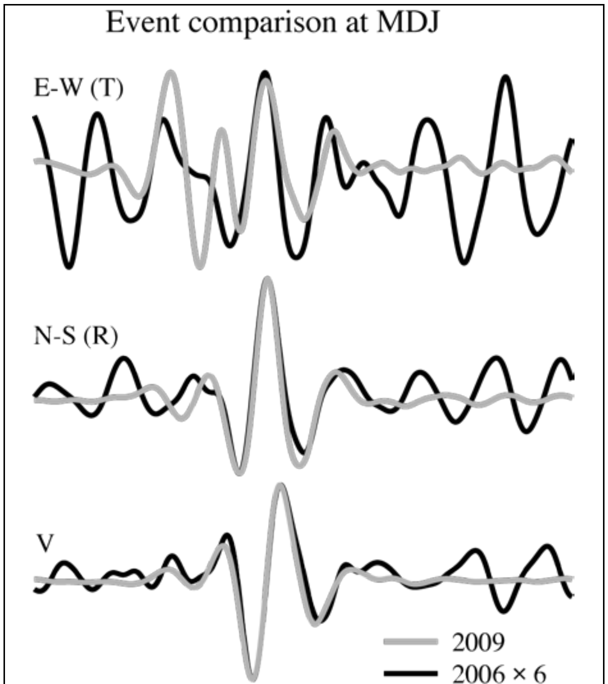

Figure 5. Raw waveforms at station MDJ for both the 2006 and 2009 North Korea events filtered between 10 and 50 sec, where the waveforms for the 2006 event are magnified by a factor of 6. Note that the azimuth to MDJ is 6˚, so the east-west and north-south components are effectively naturally rotated to the tangential and radial directions, respectively. Each trace is 100 sec long and begins 80 s after their respective origin time.

The full moment tensor inversion fits the data at 81% and yields an isotropic moment of 3.6e22 dyne-cm, and a total moment of 6.3e22 dyne-cm (M_W4.5). The deviatoric moment tensor inversion fits the data at 80% and a total moment of 3.2e22 dyne-cm (M_W4.3). If the deviatoric source is decomposed to a compensated linear vector dipole (CLVD; Knopoff and Randall, 1970) and DC sharing the same principal axes, then the source is 70% CLVD. The similarity in fits between the dominantly CLVD deviatoric source and dominantly isotropic full moment tensor shows that at shallow depths, a vertical CLVD mechanism can effectively mimic an explosion at the distances and periods analyzed here. This can be seen in the waveform comparison in Figure 6b. The full moment tensor isotropic moment is two times larger than the pure explosion indicating that the compound source of the full moment tensor solution (DC+CLVD+Isotropic) required to fit the Love waves also modifies the Rayleigh waves causing the isotropic component to increase to compensate.

As mentioned previously, some non-isotropic radiation is required to fit the source due to the observed Love waves as can be seen on the tangential component waveforms in Figure 6b. The same amount of non-isotropic energy could have been present in the recordings of the 9 October 2006 nuclear test, but were obscured due to noise.

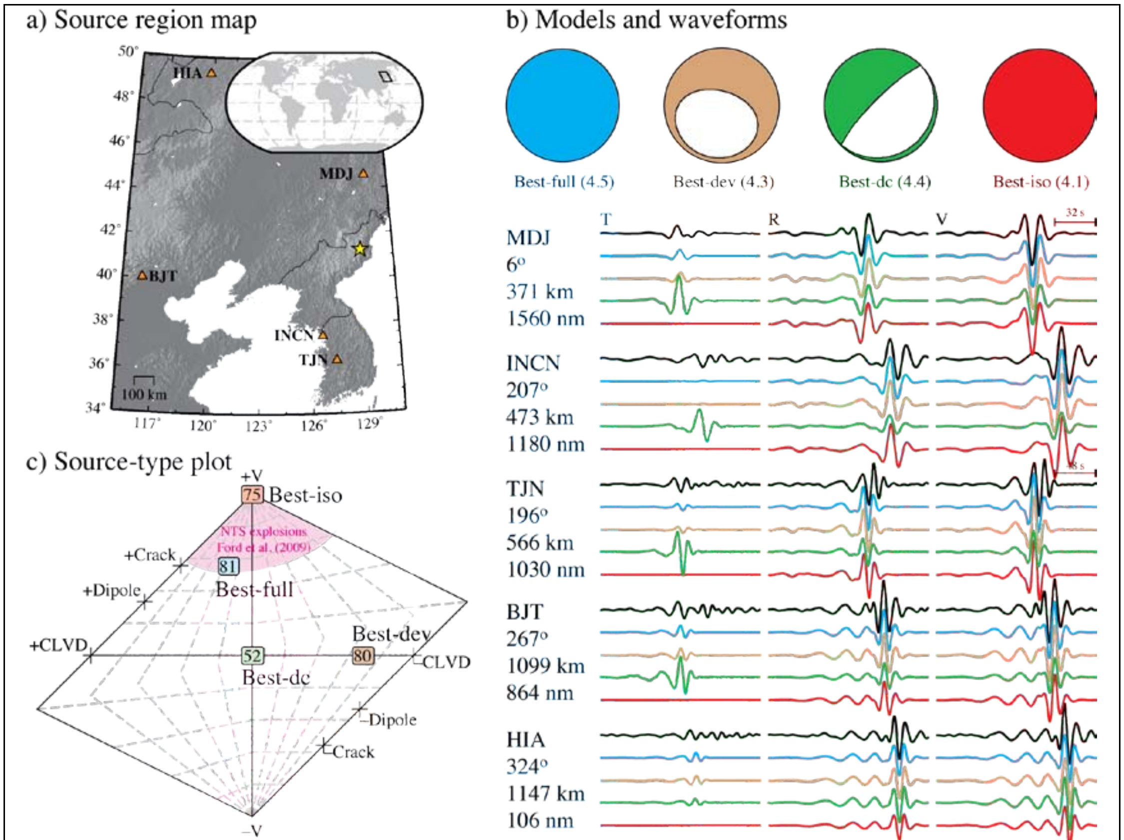

Figure 6. Source analysis of the Memorial Day Explosion, Kimchaek, North Korea (25 May 2009). a) Map of the Yellow Sea / Korean Peninsula with the North Korea explosion (star) as well as the stations used in their analysis (triangles). The region is outlined in the global inset map. b) Models (corresponding to those plotted in c) and their respective forward-predicted waveforms as a function of color compared with the actual waveforms (black line). The left, middle, and right columns are the tangential (T), radial (R), and vertical (V) displacement waveforms, respectively. The text block to the left of the waveforms gives the station name, passband period (s), azimuth, epicentral distance (km), and maximum displacement (nm). The moment magnitudes of the models are also given in parentheses. c) Source-type plot with various solutions corresponding to the models given in b) and their associated fit percent. Standard sources are also noted as well as the region of explosions at the NTS from Ford et al. (2009).

CONCLUSIONS AND RECOMMENDATIONS

Confidence in best-fit solutions for regional full-waveform moment tensor inversions is dependent on station configuration, data bandwidth, and SNR. The best way to characterize that dependence is on a case-by-case basis, where each individual event scenario is analyzed. The NSS attempts to do this characterization and is introduced and implemented in this report for the Oct 06 North Korea test, a nearby earthquake in China, and the May 09 North Korea test. A more complete description of the method is presented in Ford et al. 2009b. The theoretical network sensitivity solution provides solution confidence regions for ideal models (explosion or earthquake) with high SNR data. With this type of network sensitivity solution, one can learn if the station configuration and bandwidth is sufficient to resolve a given model. The actual network sensitivity solution assesses confidence using the actual data from the event. Goodness-of-fit for each model is parameterized with a percent variance reduction (VR), where the complete VR space can be mapped out on a source-type plot and the well-fit region of solutions is defined by a chosen threshold VR.

The theoretical network sensitivity solutions for the North Korea tests show a trade-off between CLVD and explosion, but the well-fit solution space is separated from a double-couple, indicating that an anomalous event can be resolved. In the case of the North Korea tests, a specific configuration using the very distant station BJT is required to rule out a DC solution. With some additional data weighting, the actual network sensitivity solution of the North Korea test also shows a tight region of well-fit solutions clustered between an opening crack and an explosion, though with the addition of just one more imaginary station, this region is made much smaller (Ford et al., 2009b). The network sensitivity solutions for the earthquake in China provide high confidence in the best-fit solution, which is indistinguishable for a double-couple.

Modeling of low-frequency, regional distance waveforms identifies the 2009 event as primarily an explosion source. Comparison of pure explosion and pure double-couple models indicate that the simpler explosion model fits the waveform data substantially better than the higher degree of freedom double-couple model. While the source type is well determined, the isotropic moment of the full moment tensor inversion has some uncertainty and the M_W is between 4.4 and 4.6. The preferred scalar moment for the event is the isotropic moment of 1.8e+22 dyne-cm (M_W 4.1) of the pure explosion case. However, there are Love waves observed at several stations indicating that the source must have some non-isotropic component. This component could have been present in the previous 2006 test, but was masked by the noise.

ACKNOWLEDGEMENTS

We thank Bruce Julian for scripts to make the source-type plots.

REFERENCES

Bowers, D. and J. A. Hudson (1999). Defining the scalar moment of a seismic source with a general moment tensor, *Bull. Seismol. Soc. Am*. 89: (5), 1390–1394.

Dreger, D. S. , S. R. Ford, and W. R. Walter (2008). Source analysis of the Crandall Canyon, Utah, mine collapse, *Science,* 321: 217.

Ford, S., D. Dreger, and W. Walter (2008). Source Characterization of the August 6, 2007 Crandall Canyon Mine Seismic Event in Central Utah, *Seismol. Res. Lett*. 79: 637–644.

Ford, S. R., D. S. Dreger, and W. R. Walter (2009a). Identifying isotropic events using a regional moment tensor inversion, *J. Geophys. Res*. 114: B01306, doi:10.1029/2008JB005743.

Ford, S. R., D. S. Dreger, and W. R. Walter (2009b). Network sensitivity solutions for regional moment tensor inversions, *Bull. Seismol. Soc. Am.,* Submitted.

Hudson, J. A., R. G. Pearce, and R. M. Rogers (1989). Source type plot for inversion of the moment tensor, *J. Geophys. Res*. 9: (B1), 765–774.

Jechumtalova, Z. and J. Sileny (2001). Point-source parameters from noisy waveforms: Error estimate by Monte-Carlo simulation, *Pure Appl. Geophys*. 158: 1639–1654.

Koper, K. D., R. B. Herrmann, and H. M. Benz (2008). Overview of open seismic data from the North Korean Event of 9 October 2006, *Seism. Res. Lett*. 79: (2), 178–185; doi:10.1785/gssrl.79.2.178.

Knopoff, L. and M. J. Randall (1970). The compensated linear-vector dipole; a possible mechanism for deep earthquakes, *J. Geophys. Res*. 75: (26), 4957–4963.

ODNI, Office of the Director of National Intelligence (2006). News Release No. 19-06, www.dni.gov/announcements/20061016_release.pdf

Riedesel, M. and T. H. Jordan (1989). Display and assessment of seismic moment tensors, *Bull. Seismol. Soc. Am*. 79: 85–100.

Roessler D, F. Krueger, and G. Ruempker (2007). Inversion for seismic moment tensors in anisotropic media using standard techniques for isotropic media. *Geophys. J. Int.* 169:136–148.

Sileny, J. (1998). Earthquake source parameters and their confidence regions by a genetic algorithm with a 'memory', *Geophys. J. Int*. 134: 228–242.

Sileny, J. (2004). Regional moment tensor uncertainty due to mismodeling of the crust, *Tectonophysics* 383: 133–147.

Sileny, J., P. Campus, and G. F. Panza (1996). Seismic moment tensor resolution by waveform inversion of a few local noisy records; I, Synthetic tests, *Geophys. J. Int*. 126: 605–619.

Sileny, J., G. F. Panza, and P. Campus (1992). Waveform inversion for point source moment tensor retrieval with variable hypocentral depth and structural model, *Geophys. J. Int*. 109: 259–274.

Walter, W., E. Matzel, M. Pasyanos, D. Harris, R. Gok, and S. Ford (2007). Empirical Observations of Earthquake-Explosion Discrimination Using P/S Ratios and Implications for the Sources of Explosion S-Waves, in *Proceedings of the 29th Monitoring Research Review: Ground-Based Nuclear Explosion Monitoring Technologies*, LA-UR-07-5613, Vol. 1, pp. 684–693,

Weber, Z. (2006). Probabilistic local waveform inversion for moment tensor and hypocentral location, *Geophy. J. Int*. 165: 607–621.